Spherocytic shift of red blood cells during storage provides a quantitative whole cell–based marker of the storage lesion

Camille Roussel,[1,3] Michaël Dussiot,[3] Mickaël Marin,[2] Alexandre Morel,[3] Papa Alioune Ndour,[1] Julien Duez,[1] Caroline Le Van Kim,[2] Olivier Hermine,[3,4] Yves Colin,[2] Pierre A. Buffet,[1] and Pascal Amireault[2,3]

BACKGROUND: Storage lesion may explain the rapid clearance of up to 25% of transfused red blood cells (RBCs) in recipients. Several alterations affect stored RBC but a quantitative, whole cell–based predictor of transfusion yield is lacking. Because RBCs with reduced surface area are retained by the spleen, we quantified changes in RBC dimensions during storage.

STUDY DESIGN AND METHODS: Using imaging flow cytometry we observed the dimension and morphology of RBCs upon storage, along with that of conventional biochemical and mechanical markers of storage lesion. We then validated these findings using differential interference contrast (DIC) microscopy and quantified the accumulation of microparticles (MPs).

RESULTS: Mean projected surface area of the whole RBC population decreased from 72.4 to 68.4 μm^2, a change resulting from the appearance of a well-demarcated subpopulation of RBCs with reduced mean projected surface (58 μm^2, 15.2%-19.9% reduction). These "small RBCs" accounted for 4.9 and 23.6% of all RBCs on Days 3 and 42 of storage, respectively. DIC microscopy confirmed that small RBCs had shifted upon storage from discocytes to echinocytes III, spheroechinocytes, and spherocytes. Glycophorin A–positive MPs and small RBCs appeared after similar kinetics.

CONCLUSION: The reduction in surface area of small RBCs is expected to induce their retention by the spleen. We propose that small RBCs generated by MP-induced membrane loss are preferentially cleared from the circulation shortly after transfusion of long-stored blood. Their operator-independent quantification using imaging flow cytometry may provide a marker of storage lesion potentially predictive of transfusion yield.

Eighty-five million patients receive a red blood cell (RBC) transfusion each year worldwide (World Health Organization). The complex management of the transfusion process is facilitated by the possibility to store RBC for up to 42 days after blood collection (less commonly 35 days in some countries). During this 6-week-long period, a series of modifications that alter RBC have been described, collectively referred as

"storage lesion," suggesting that RBC quality does not remain stable during hypothermic storage. Despite progressive improvement of storage conditions in blood banks (use of plastic bags and optimized additive solutions, leukoreduction), the storage lesion remains a matter of concern as it is responsible for the rapid clearance of up to 25% of transfused RBCs over a few hours, thereby reducing transfusion yield.[1,2] This proportion of cleared RBCs increases with storage duration and displays marked interdonor variabilities.

So far, relatively little has been demonstrated regarding the clinical significance of this rapidly cleared population of transfused RBCs. Although correlations have been observed between duration of storage and adverse events,[3-5] recent clinical trials have been reassuring about potential harmful effects related to the transfusion of "older" RBCs in current clinical practice.[6,7] However, these studies did not assess the impairment of transfusion yield and were not designed to explore the last third of the storage period (Day [D]28 to D42) with adequate statistical power. Furthermore, studies are still lacking for specific patient populations such as fragile or chronically transfused patients, who are particularly vulnerable to microcirculatory impairment or iron overload and who could benefit the most from improvement of transfusion yield.

The Food and Drug Administration (FDA) threshold to approve a preparation and storage process of RBCs is a maximum 1% in vitro hemolysis (0.8% in European regulations[8]) and a 24-hour in vivo recovery of at least 75% after reinfusion of autologous radiolabeled RBC in healthy volunteers, 42 days after donation.[9] This in vivo measurement of posttransfusion survival remains essential because so far, no in vitro marker can accurately predict the viability of stored RBCs.[10,11] Even though measurement of other variables such as concentrations of adenosine triphosphate (ATP), 2,3-diphosphoglycerate acid, glucose, lactate, and RBC deformability are also routinely performed, no decisional thresholds have been determined and, accordingly, none of them is an absolute criterion for approval.[1] Numerous published observations have reported strong evidence about the accumulation of biomechanical, molecular, and morphologic changes associated with storage duration.[12] None of these variables is, however, a reliable predictor of posttransfusion recovery, as they generally reflect the alterations of a global population but cannot discriminate RBCs that will be able to circulate in the recipient from those that will be cleared. An optimal quantitative marker of transfusion in vivo recovery should therefore identify a subpopulation that matches the proportion of RBC exposed to early premature clearance.

Because it retains and eliminates RBC displaying surface or mechanical alterations, the spleen is expected to contribute significantly to the premature clearance of transfused RBCs. A specific characteristic of this organ is its ability to sense purely mechanical alterations of RBCs even in the absence of surface modifications. In some inherited RBC disorders, such as hereditary spherocytosis, a tight relationship between the morphology and the deformability of RBCs has been demonstrated.[13] Surface area-to-volume ratio is a major determinant of RBC deformability and of their ability to circulate[14,15] as it allows normal discocytes (8 μm in diameter) to deform enough to navigate along 4- to 6-μm-wide microvessels and to cross 1- to 2-μm-wide interendothelial slits in the spleen. Experiments in mice have confirmed the rapid removal from circulation of spherical RBCs upon reinfusion[16,17] and human studies have shown a correlation between the shape of RBCs and their persistence in circulation.[18] In addition, ex vivo perfusion of human spleens have shown a strong positive correlation between the number of RBCs retained in the spleen and the proportion of projected surface area they had lost.[19] Retention was greater than 90% for RBCs that had lost more than 18% of their projected area. This result confirms the existence of a "splenic clearance threshold" based on biomechanical alterations. A recent in vitro study using salicylate-exposed human RBCs also correlated RBC morphologic alterations and their ability to circulate in a microfluidic device.[20] Thus, data suggest that morphologic changes could trigger clearance of RBCs if the intensity of these alterations reaches the spleen-sensing threshold. We hypothesized that RBC morphologic changes occurring during storage would result predominantly from membrane loss and decrease in surface area, an alteration that may trigger splenic entrapment and could lead to premature clearance of markedly altered RBCs.

In this study, we used imaging flow cytometry (ImageStream X Mark II, AMNIS part of EMD Millipore) to characterize the dimensions and morphology of RBCs stored in blood bank conditions, on D3, D21, D28, D35, and D42 of the storage period and to assess the accumulation of microparticles (MPs). Imaging flow cytometry enables a simultaneous high-speed multispectral imaging of cells, as it combines the speed and phenotyping capacity of conventional flow cytometry to analyze a very high number of events, with a detailed and objective exploration of cell morphology. This exploration was performed in the context of a comprehensive study of storage lesion where biochemical, metabolic, and biomechanical characteristics of stored RBC were assessed in parallel.

MATERIALS AND METHODS

Blood collection and sampling of RBCs

Leukoreduced RBCs in SAG-M from six healthy donors were supplied by the Etablissement Français du Sang (French Blood Service) 2 days after blood collection. All units were stored in optimal blood bank conditions,

between 2 and 6°C and for 42 days, according to regulations. Samples were aseptically collected on 2 consecutive days (D3-4, D20-21, D27-28, D34-35, and D41-42 of storage) to perform all experiments. Because preliminary observations had shown little morphologic variations during the first 3 weeks of storage (Fig. S1, available as supporting information in the online version of this paper), weekly analysis of variables started on D20 and D21, with a baseline determination upon reception of concentrates on D3 and D4.

RBC dimensions and morphology assessment by imaging flow cytometry

Imaging flow cytometry (ImageStream X Mark II, AMNIS part of EMD Millipore) was performed to determine RBC dimensions and morphology by using brightfield images (60× magnification) processed with computer software (IDEAS v6.2, AMNIS part of EMD Millipore). Focused cells were selected using gradient RMS and single cells were gated using area and aspect ratio. Finally, front views were selected by the circularity feature (mask "Object"). At least 6000 front views of focused single cells were used for analysis at each time point. Normalized frequency plot of projected surface area and aspect ratio (ratio of the width and height of the RBC) were assessed using the mask "Object." Stored RBCs were suspended at 1% hematocrit (Hct) just before acquisition (INSPIRE software, AMNIS part of EMD Millipore) in a Krebs-albumin solution (Krebs-Henseleit buffer, Sigma-Aldrich) modified with 2 g of glucose, 2.1 g of sodium bicarbonate, 0.175 g of calcium chloride dehydrate, and 5 g of lipid-rich bovine serum albumin (AlbuMAX II, Thermo Fisher Scientific) for 1 L of sterile water (pH 7.4).

Differential interference contrast microscopy

RBCs were washed in Krebs-albumin solution to remove storage solution and suspended in Krebs-albumin to obtain a final dilution at 0.014% of Hct. The diluted RBCs were added to an Ibidi flow chamber (μ-Slide I 0.4 Luer uncoated, Ibidi) and kept for 10 minutes to allow sedimentation. Differential interference contrast (DIC) images were acquired using a confocal microscope (ZEISS LSM 700, Objectif Plan APOCHROMAT 40X/1.3 oil, Carl Zeiss). Twenty images (representing 600 to 1000 RBCs) for each sample were acquired, anonymized, and randomized to allow blind analysis. Results are presented according to the Bessis classification[21] adapted for DIC microscopy.[22]

Hemolysis, Hct, and mean corpuscular volume measurement

Total and free hemoglobin (Hb) were measured with a plasma and low-Hb spectrophotometer (HemoCue). Percentage of hemolysis was calculated using the formula

$$[Free\ Hb]/[Total\ Hb]) \times (100 - Hct).$$

Hct was determined by microcentrifugation technique using a micro/Hct centrifuge (Microfuge NF048, NÜVE). The mean of two independent measures was used for analysis. Mean corpuscular volume (MCV, μm^3) was established using a hematologic device (ABX Pentra 80, HORIBA).

Biochemical variables

Supernatant was collected after centrifugation (1500 × g, 15 min) and frozen at −80°C until analysis. Biochemical variables (potassium, sodium, chloride, lactate, glucose, and iron concentrations) were assessed with a multiparametric automat (Model AU400, Olympus).

Determination of ATP concentration

ATP concentration was determined by luminescence assay using a commercial kit (ATPlite, PerkinElmer). Samples were measured in duplicate and according to the manufacturer's procedure. ATP concentration was then computed (μmol/dL) using the standard curve and normalized with Hb concentration (μmol/g Hb).

RBC elongation index measurement

RBC deformability was evaluated by the elongation index (EI) measured by ektacytometry as described previously,[23] using a laser-assisted optical rotational cell analyzer (LORRCA, Mechatronics). EI was defined as the ratio of the difference between the two axes of the ellipsoidal diffraction pattern and the sum of these two axes. The control was frozen RBCs from a healthy donor, thawed the day of the experiment; the same RBC sample was used for all experiments to minimize potential variability.

Osmotic fragility test

RBC osmotic fragility was determined as previously described.[24] Briefly, RBCs were washed in phosphate-buffered saline (PBS), incubated for 45 minutes in hypotonic $NaCl-PO_4$ solutions (equivalent to NaCl solutions, ranging from 0% to 0.9%), and centrifuged (800 × g, 5 min). Absorbance of the released Hb was measured at 540 nm using a spectrophotometer and percentage of hemolysis for each salt concentration was calculated (DO value measured for condition Eq NaCl 0% corresponding to 100% hemolysis).

Determination of MPs concentration

Supernatant containing MPs was collected after centrifugation (1500 × g, 15 min) and frozen at −80°C until analysis. Before staining, all buffers were sterile filtered twice with a 0.22-μm filter. CD235a-PE (BD PharMingen), CD45-FITC (Ebiosciences), and CD41-Pacific Blue (Biolegend) antibodies were diluted at a final concentration of

1:25 directly in MP preparations. Samples were incubated for 60 minutes in the dark at room temperature and then washed in PBS (centrifugation at $17,000 \times g$ for 10 min) and resuspended in 100 μL of PBS. Images were acquired on an imaging flow cytometer (ImageStream X Mark II, AMNIS part of EMD Millipore) at 60× magnification. All lasers (488, 561, 405, and 785 nm) were used at full power. A total of 100,000 events were acquired for each condition. To calculate compensations, single staining matrix for each fluorochrome was done. MP gating strategy was used as previously described.[25] Concentration of MP was assessed using IDEAS software and the background staining emitted by the antibody mix alone was subtracted.

RESULTS

Kinetics of conventional markers are consistent with published observations

We analyzed the kinetics of biochemical, metabolic, and biomechanical characteristics of stored RBCs from six donors (Fig. 1). Mean hemolysis level on D42 was 0.32% (range, 0.17%-0.44%) and did not exceed the 0.8% limit defined by European regulations at the end of storage (Fig. 1A), which confirms the appropriate quality of RBCs used in this study. Evolution of MCV, intracellular ATP level, and plasma concentrations of ions and metabolites were consistent with published observations (Fig. 1A). The percentage of hemolysis as function of the extracellular osmolarity shifted to the right, denoting the appearance of osmotically sensitive RBCs upon storage (Fig. 1B). Deformability, evaluated by maximum elongation index (shear stress 30 Pa) measured by ektacytometry, also decreased mildly with storage duration (Fig. 1C). These two results suggest the accumulation of a subpopulation of RBCs with an increased susceptibility to storage lesion, particularly during the last 2 weeks of storage.

Imaging flow cytometry determines robust distribution patterns of the projected surface area of large populations of RBCs

Using imaging flow cytometry, we analyzed the distribution of the projected surface area of stored RBCs (six donors) on normalized frequency plots, between D3 and D42 of storage (at least 6000 RBCs/sample). Projected surface area exhibited a Gaussian or nearly Gaussian distribution for all donors on D3 (Fig. 2A). Mean surface area was 72.4 μm^2 (70.5-74.4 μm^2) and was distributed approximately from a minimum of 40 μm^2 to a maximum of 100 μm^2. This pattern was similar to those of fresh RBCs from healthy donors collected just before analysis and resuspended in the same buffer (superimposed black line, Fig. 2A). Of note, this surface represented approximately 50% of the whole normal RBC surface. This was consistent with previous observations based on micropipette

aspiration technique that measured a mean surface area of 134 μm^2 for discocytes.[26]

The unimodal distribution of projected surface area undergoes a bimodal segregation upon RBC storage

Mean projected surface area of the whole RBC population significantly decreased from 72.4 μm^2 (70.5-74.4 μm^2) on D3 to 68.4 μm^2 (63.9-74.0 μm^2) on D42 (Fig. 2B) but this reduction was mainly due to the progressive emergence of a RBC subpopulation of low surface area. Indeed, in 5 of 6 units, the surface area distribution became progressively bimodal upon storage with the appearance of a well-demarcated subpopulation of smaller RBCs (Fig. 2A). Segregating "small RBCs" (left of the dashed line, Fig. 2A) from "normal RBCs" (right of the dashed line, Fig. 2A) was performed independently for each donor, using the nadir of the bimodal frequency histograms as the gating boundary. The surface distribution histogram on D3 crossed the surface distribution histogram on D42 exactly at this nadir in all donors (Fig. 2A), confirming the robustness of this gating procedure. For all donors, the small RBC subpopulation accumulated upon storage from 4.9% (1.1%-8.5%) on D3 to 23.6% (4.9%-38.5%) on D42 ($p < 0.05$, Fig. 2C), with marked interdonor variability. Remarkably, Donor 5 displayed a low proportion of small RBCs on D42 (4.9%) when compared to other donors. Increase in the proportion of the small RBC subpopulation was markedly faster during the last third of the storage period (+14% between D28 and D42) than during the first two-thirds of this period (+4.8% between D0 and D28).

The subpopulation of small RBCs corresponds to morphologically altered RBCs

Morphologic analysis of imaging flow cytometry brightfield images using categories based on an adaptation of the Bessis classification (Fig. 4A) revealed that echinocytes III, spheroechinocytes, and spherocytes accounted for 88% (73%-96%) of the small RBC subpopulation (Fig. 3A, left panel). Conversely, 89% (82%-94%) of RBCs with a normal surface area were discocytes, echinocytes I, and echinocytes II (Fig. 3A, right panel). Moreover, the circularity of the small RBC subpopulation increased with storage duration while the projected surface area decreased. Taken together, these data showed an increased sphericity in the subpopulation of small RBCs, reflecting an increase in the proportion of spheroechinocytes and spherocytes during storage. Remarkably, surface area and aspect ratio of normal RBC did not vary during the same storage period (Fig. 3B).

Reference morphologic analysis of RBCs using differential interference phase contrast microscopy validates imaging flow cytometry findings

We next evaluated the evolution of RBC morphology during storage by DIC microscopy and compared these
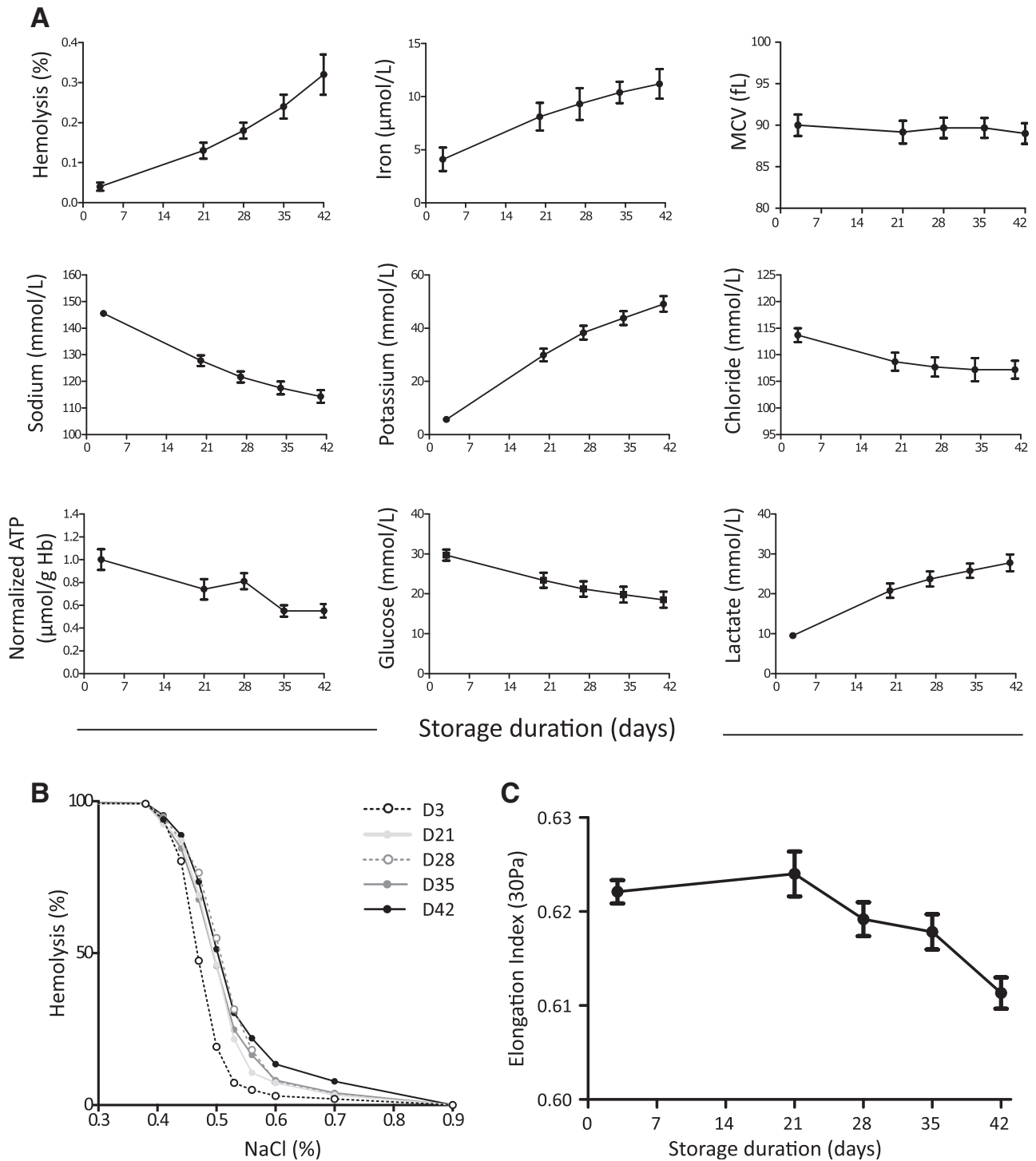
Fig. 1. Kinetics of conventional markers of storage lesion. (A) Kinetics of hemolysis, iron, sodium, potassium, chloride, glucose, lactate, and ATP concentrations in RBCs and of MCV (n = 6, mean ± SEM). (B) Osmotic fragility test: evolution of the percentage of hemolysis as function of the extracellular osmolarity (% equivalent NaCl) upon storage (n = 6, mean). (C) Maximum EI measured by ektacytometry (shear stress 30 Pa) upon storage (n = 6, mean ± SEM).

observations to those obtained by imaging flow cytometry. Both approaches used the same morphologic categories adapted from Bessis classification, namely, discocytes, echinocytes (I, II, and III), stomatocytes, spheroechinocytes, and spherocytes. Typical images of RBCs from each morphologic category are shown in Fig. 4A. DIC
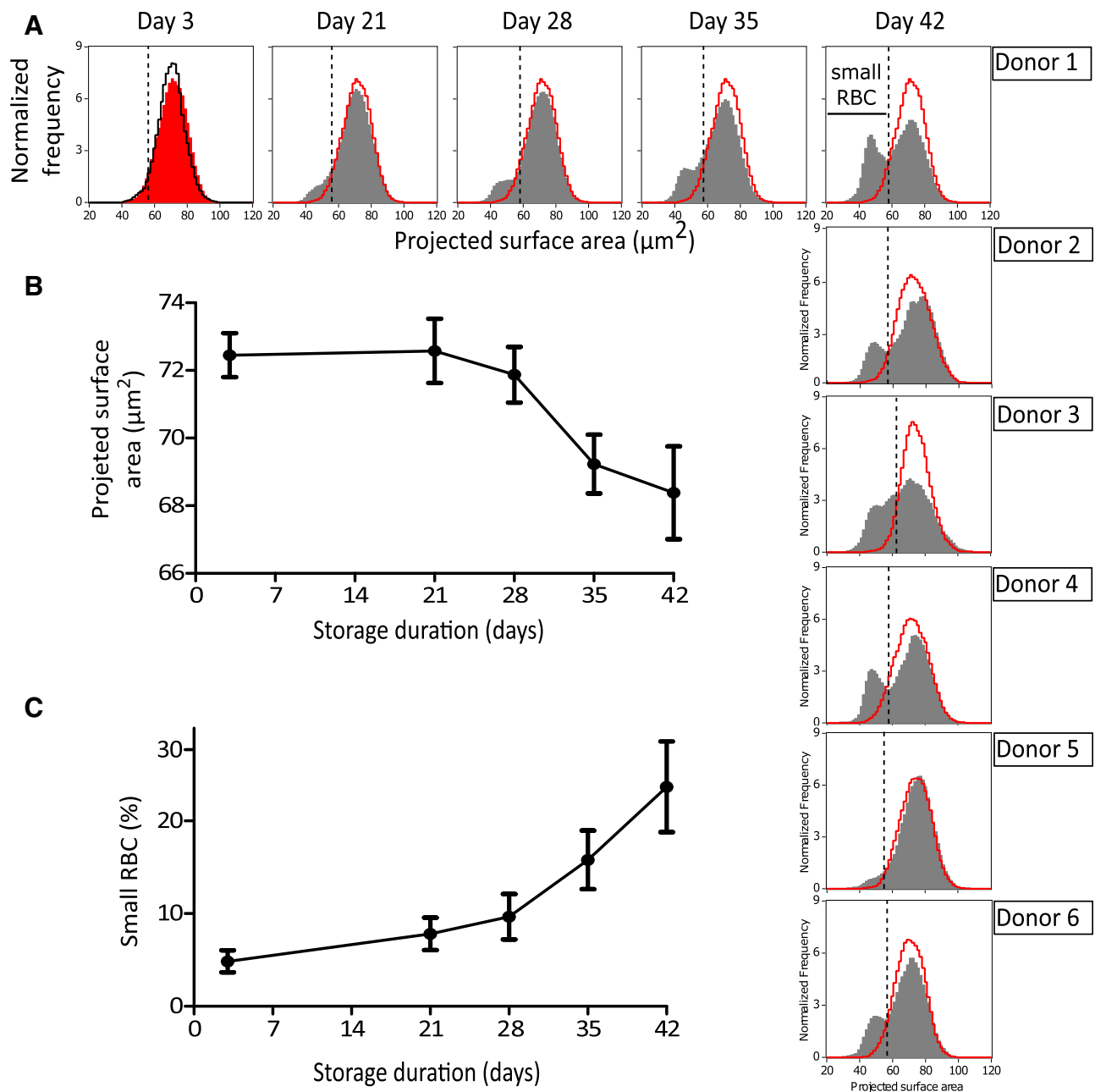
Fig. 2. Imaging flow cytometry identifies a well-demarcated subpopulation of small RBCs that accumulates during storage. (A) Typical evolution of projected surface area on normalized frequency plot for one donor between D3 and D42 of the storage period (horizontally) showing the apparition of a well-demarcated subpopulation of small RBCs, at the end of the storage period (D42), for the six donors (vertically), highlighting a great interdonor variability. The superimposed red line shows the profile of each donor's RBC population at the beginning of storage (D3). The black line shows the profile of a typical fresh RBC population. Dashed vertical lines define gating of the small RBC subpopulation for each donor. (B) Evolution of projected surface area for front views of focused single RBCs (n = 6, mean ± SEM) and (C) evolution of the proportion of the small RBC subpopulation upon storage (n = 6, mean ± SEM). [Color figure can be viewed at wileyonlinelibrary.com]

microscopy observations confirmed storage-induced morphologic alterations (Fig. 4B). The relative proportion of each category was quantified at each evaluation point upon storage (Fig. 4C). Proportion of discocytes decreased

from 60.1% (43.2%-69.4%) at D3 to 33.7% at D42 (13.8%-51%) while that of echinocytes steadily increased (Fig. 4C, lower panel). The proportion of stomatocytes started to decrease from D21 to reach 6.8% of the population at the
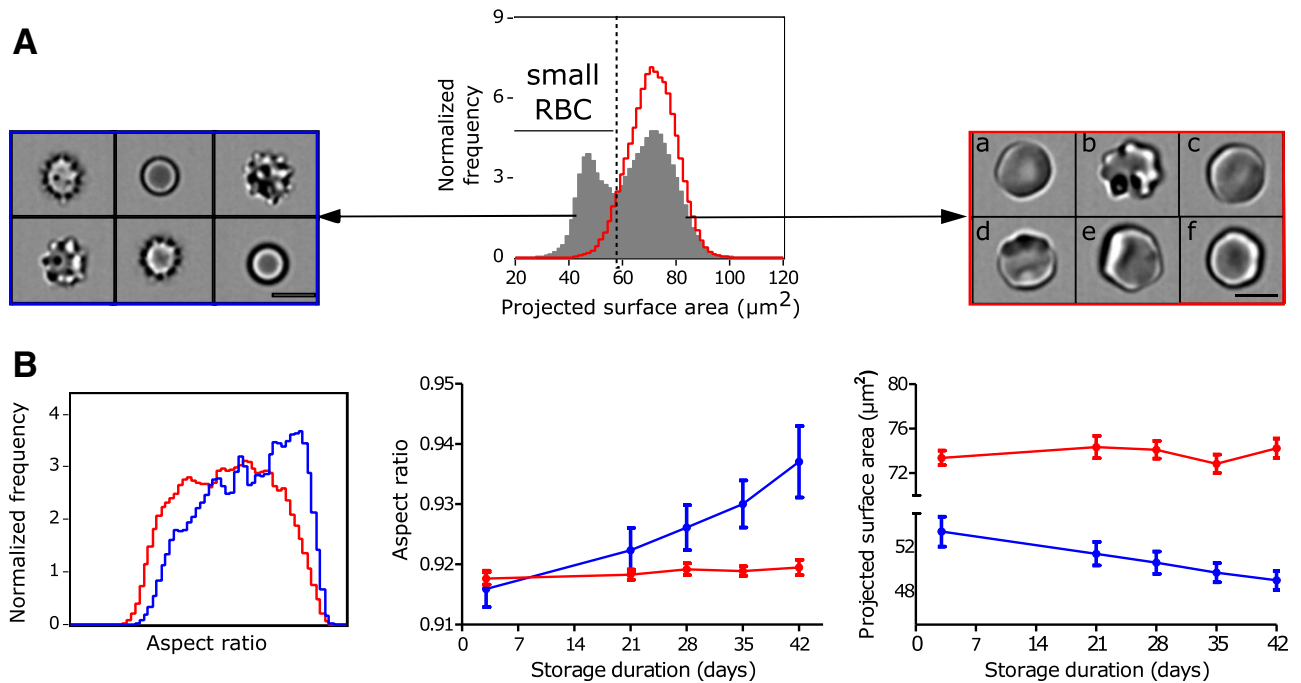
Fig. 3. The subpopulation of small RBCs contains essentially spherocytes, spheroechinocytes, and echinocytes III. (A) Typical ImageStream brightfield images of small RBCs (left panel) showing spherocytes (b and f), spheroechinocytes (a and e), and echinocytes III (a and d) and normal-sized RBCs (right panel) showing discocytes (a and c), echinocytes I (e and f), and echinocytes II (b and d). (B) Typical aspect ratio frequency histogram of small RBCs (blue curve) and normal RBCs (red curve) on D42 (left panel). Evolution of aspect ratio (middle panel) and projected surface area (right panel) of the small RBCs (blue line) and normal RBCs (red line) subpopulations upon storage. [Color figure can be viewed at wileyonlinelibrary.com]

end of storage (D42). The proportion of echinocytes (II and III), spherocytes, and spheroechinocytes increased more rapidly after D28 and D35, respectively (Fig. 4C). There was a very strong correlation between the proportion of small RBCs determined using imaging flow cytometry and the proportion of echinocytes III, spherocytes, and spheroechinocytes determined by DIC (correlation squared coefficient = 0.91; Figs. 2C, 5A, B). Moreover, similar proportions of these three categories were found both in the small RBC gate (imaging flow cytometry) and in DIC analysis (Fig. 5C).

RBC MPs accumulate upon storage and their concentration correlates with that of small RBCs

MPs in the supernatants of RBCs were quantified at each time point. Imaging flow cytometry, which is at least as sensitive as conventional flow cytometry, was used to detect MPs.[25,27] CD45 and CD41 staining showed no accumulation of white blood cell– or platelet-derived MPs (Table 1). Glycophorin A–positive (GPA[+]) MPs accumulated slowly during the first 4 weeks of storage but then increased exponentially between D28 and D42 (Fig. 6), again with marked interdonor variability. Stored RBCs from Donor 5 showed markedly lower MP accumulation

between D3 and D42 compared to samples from other donors ($\times$3 vs. $\times$77, not shown). Interestingly, the RBCs from Donor 5 also contained a low concentration of small RBCs at the end of storage (4.9%, Fig. 2A).

DISCUSSION

Using imaging flow cytometry to characterize the dimension and morphology of RBCs upon storage, we have identified a subpopulation of small spherocytic RBCs the proportion of which increases with storage duration and varies widely between donors. Previous physiologic observations have linked morphology and mechanical retention of RBC,[16,18-20] suggesting that the small spherocytic population may be preferentially cleared by the spleen. If this hypothesis is confirmed, rapid quantification of this subpopulation of altered RBC may become a predictor of transfusion yield.

Previous observations have described morphologic alterations of RBCs during storage. Most studies used conventional microscopy (DIC or SEM) to analyze glutaraldehyde-fixed RBCs without measuring RBC dimensions.[28-30] Cell fixation on its own induces volume, morphologic changes, or both.[31-33] Morphologic
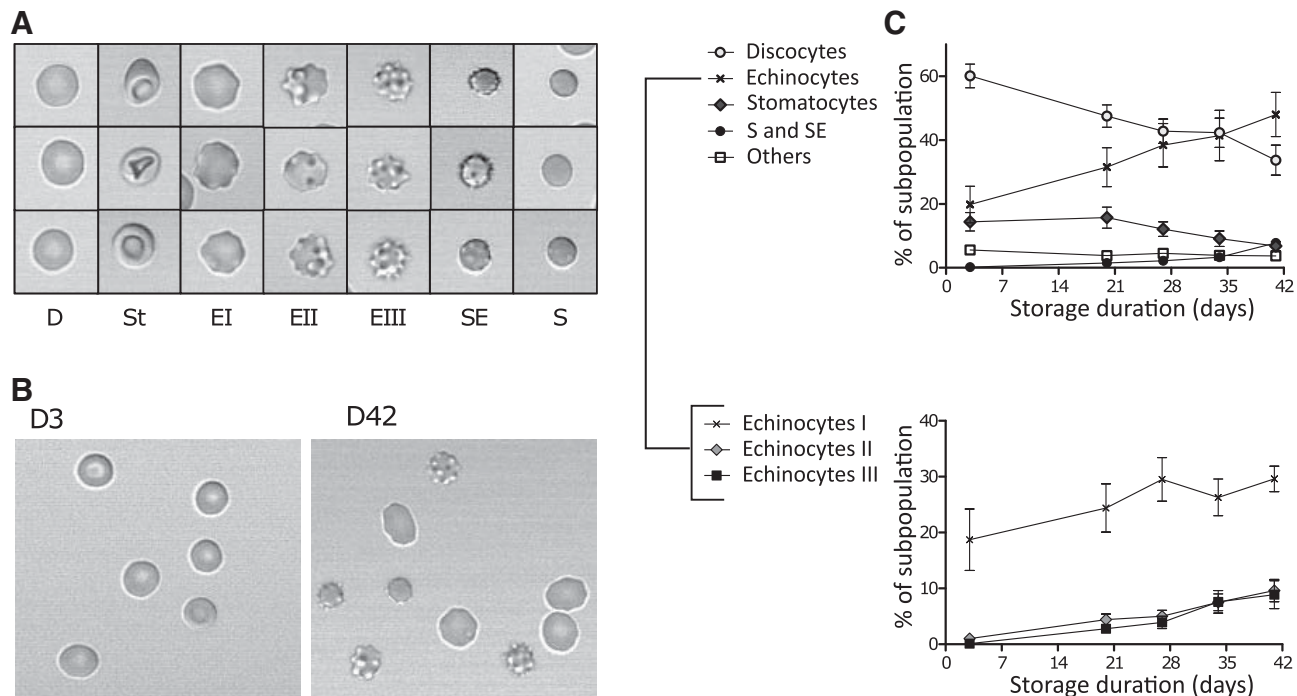
Fig. 4. DIC microscopy accurately categorizes morphologic alterations of unfixed RBCs during storage. (A) Typical images (×400 magnification) for each morphologic category were analyzed using the Bessis classification adapted for DIC microscopy: discocytes (D), stomatocytes (St), echinocytes I (EI), echinocytes II (EII), echinocytes III (EIII), spheroechinocytes (SE), and spherocytes (S). (B) Typical DIC images (×400 magnification) of RBCs on D3 (left) and D42 (right). (C) Evolution of each morphologic category (n = 6, mean ± SEM) during storage.

characterization was often limited to a distinction between "reversible" and "irreversible" alterations, where reversibility was not unequivocally defined and based on variable sets of variables. These previous studies used low-throughput and operator-dependent methods. Because fine morphologic classification of RBCs depends on the pH and composition of the suspension medium[21,34] we used Krebs-albumin solution shown in preliminary experiments to provide the best preservation of surface area including the bimodal distribution of stored RBCs, compared to serum or plasma. Imaging flow cytometry has been increasingly used to study RBC morphology and pathology.[35-37] Although it generates less precisely defined images than does conventional microscopy, the analysis of critical size and shape features on many unfixed RBCs using the IDEAS postacquisition software is rapid, objective, and reproducible. RBC morphologic categories were identified with similar efficiency using either imaging flow cytometry or classification by eye of thousands of RBCs imaged with DIC microscopy (Figs. 4 and 5). We thus provide here a robust description of morphologic alterations of unfixed RBCs stored after leukoreduction under current transfusion conditions. We also confirm that imaging flow cytometry, which combines the morphologic accuracy of conventional imaging methods

and the large-scale, operator-independent quantification power of flow cytometry, displays major technical strengths for quality control purposes in the field of transfusion medicine. The spherocytic shift of stored RBCs quantified by imaging flow cytometry is not only a potential marker, but a likely operator of poor transfusion yield.

The mechanisms leading to RBC morphologic alterations are not fully understood, but it is generally accepted that late echinocytes (echinocytes III and spheroechinocytes) progressively lose membrane through budding of microvesicles from their spicules.[22,38,39] Microvesiculation likely results from the disorganization of the membrane–cytoskeletal interaction modulated by ATP levels, cation homeostasis, and cellular metabolism, which are well-known markers of storage lesion.[12] As RBCs lose more surface than volume upon vesiculation, the result is an increased sphericity. Spherocytic RBCs no longer display the advantageous surface-to-volume ratio that enables normal discocytes to navigate unevenly along small capillaries and to cross very narrow slits in the spleen.[13,16,40] In our study echinocytes III, spheroechinocytes, and spherocytes were observed to form a subpopulation of stored RBCs with reduced projected surface area and increased sphericity. These small spherocytic RBC accumulated upon storage with a marked acceleration
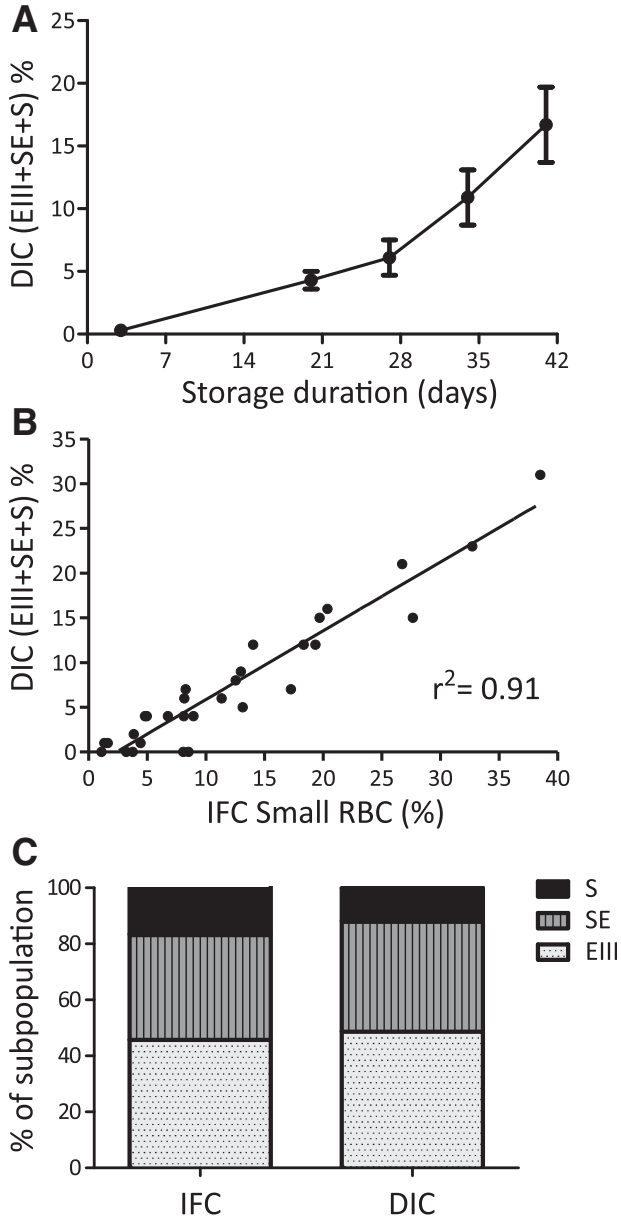
TABLE 1. Concentration of MP GPA+, CD45+, and CD41+ upon storage (n = 6)*

Days	MP GPA$^+$/μL	MP CD45$^+$/μL	MP CD41$^+$/μL
3	8,991 ± 1,451	64 ± 21	32 ± 6
21	59,995 ± 19,536	8 ± 4	40 ± 9
28	106,073 ± 39,672	32 ± 12	59 ± 10
35	267,383 ± 85,344	33 ± 15	68 ± 7
42	695,632 ± 163,272	38 ± 18	62 ± 16

* *Data are reported as mean ± SEM.
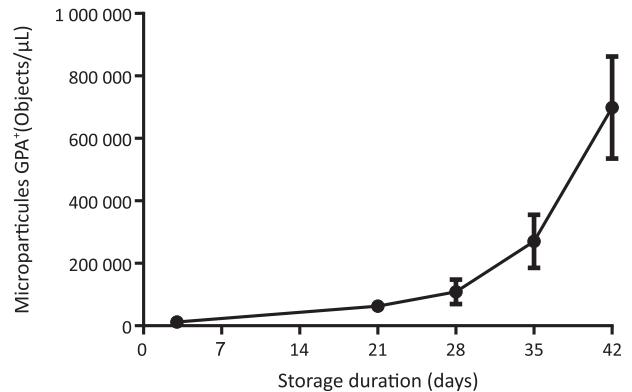
Fig. 6. GPA$^+$ MP accumulate upon storage. Concentration of GPA$^+$ MPs upon storage (n = 6, mean ± SEM).

Fig. 5. DIC microscopy validates imaging flow cytometry findings. (A) Proportions of echinocytes III (EIII), spheroe-chinocytes (SE), and spherocytes (S) upon storage using DIC microscopy (n = 6, mean ± SEM). (B) Correlation between proportions of EIII + SE + S determined by DIC microscopy and the proportion of small RBCs quantified by imaging flow cytometry (IFC) during storage. (C) Relative proportions of EIII, SE, and S identified by imaging flow cytometry (left his-togram, IFC) or DIC microscopy (right histogram, DIC) in samples of all donors on D42.

after D28. Accumulation of GPA$^+$ MPs in stored concentrates showed similar kinetics in agreement with the hypothesis that these MP are released from spicules of RBC undergoing the spherocytic shift (echinocytes III,

shperoechinocytes). Future clinical studies will determine whether membrane surface of small spherocytic RBCs is restored once they are in circulation or whether their membrane loss is irreversible and induces mechanical clearance from circulation.

Previous studies using imaging flow cytometry have unequivocally shown that surface area loss of RBCs is almost linearly correlated with splenic retention.[19] The small RBC subpopulation exhibited, at each time point, and for all donors, a 20% decrease in their surface area when compared to normal RBCs. This decrease is below the splenic retention threshold defined in previous obser-vations[16,19] and should result in an enhanced splenic entrapment of these altered RBCs. The subpopulation of small spherocytic RBCs accounted for 23.6% of the whole RBC population on D42, a proportion strongly reminis-cent of the FDA-accepted threshold for the proportion of RBCs cleared from the circulation in the 24 hours after transfusion.[1] Indeed, these RBC labeling studies have shown that a proportion of transfused RBCs is rapidly cleared while those that persist in circulation beyond 24 hours display an elimination half-life similar to that of normal RBCs.[2,41] This further supports the hypothesis that a discrete RBC subpopulation with an increased suscepti-bility to storage lesion contributes significantly to the ini-tial drop in transfused labeled RBCs. Band 3 clustering and CD47 expression level or modifications at the surface of altered RBC have been proposed as potential markers

predicting the clearance of altered RBCs from circulation.[42-44] Phosphatidylserine exposition, a quantifiable and recognized prophagocytic signal has been shown to increase during storage.[45-47] However, the proportion of phosphatidylserine-exposing RBCs on D35 to D42 of storage (between 0.02 and 7%) is markedly lower than the rapidly cleared RBC subpopulation.[45-47] In addition to surface alteration, shape and rigidity of RBCs can trigger their retention in the spleen and be sensed by macrophages thereby inducing phagocytosis.[48] Taken together, these observations point to small RBCs (as defined in this report) as strong contributors to reduced transfusion yield when "older blood" is transfused[2] either independently from surface alterations or synergistically with them. Why only a relatively small subpopulation of stored RBC is markedly altered by storage lesion and whether surface marker and/or morphologic features are involved in the clearance of altered RBCs remains to be explored in detail at the cellular and molecular level.

Our study showed that major morphologic changes occurred after 4 weeks of storage while only minor modifications were observed on D3 and D21. This is consistent with in vitro assays showing that irreversible alterations generally occurred within the last 2 weeks of storage.[12,49] Recent clinical trials showed similar outcomes in patients transfused either with "short-" (<7 days) or "long-term-stored" RBCs (22-28 days depending on the studies). However, these studies did not investigate the impact of storage for more than 4 weeks with adequate power.[6,7] These major trials were therefore not designed to exclude a potential negative impact of transfusion with concentrates containing proportions of small spherocytic RBCs higher than 20%, and did not include precise estimates of transfusion yield. We propose that these outcomes deserve specific exploration. In this study, we have clearly demonstrated that imaging flow cytometry enables definition and easy quantification of a discrete subpopulation of storage-induced small spherocytic RBCs. Future investigations will aim at determining the ability of this small RBC population to escape splenic retention either ex vivo[50,51] or in vivo.[2] If its premature clearance is confirmed, this peculiar subpopulation may become a solid candidate to predict transfusion yield. Marked quality variations may exist between donors and, in our small cohort, we observed wide variation in the proportion of small spherocytic RBC at the end of storage (from 4.9% to 38.5%). Validation of such a simple predictive quality marker of RBC concentrates may enable the selection of optimal RBCs for transfusion of fragile or chronically transfused patients.

CONFLICT OF INTEREST

The authors have disclosed no conflicts of interest.

REFERENCES

1. Dumont LJ, AuBuchon JP. Evaluation of proposed FDA criteria for the evaluation of radiolabeled red cell recovery trials. Transfusion 2008;48:1053-60.

2. Luten M, Roerdinkholder-Stoelwinder B, Schaap NP, et al. Survival of red blood cells after transfusion: a comparison between red cells concentrates of different storage periods. Transfusion 2008;48:1478-85.

3. Koch CG, Li L, Sessler DI, et al. Duration of red-cell storage and complications after cardiac surgery. N Engl J Med 2008; 358:1229-39.

4. Goel R, Johnson DJ, Scott AV, et al. Red blood cells stored 35 days or more are associated with adverse outcomes in high-risk patients. Transfusion 2016;56:1690-8.

5. Kim Y, Amini N, Gani F, et al. Age of transfused blood impacts perioperative outcomes among patients who undergo major gastrointestinal surgery. Ann Surg 2016;265:103-10.

6. Lacroix J, Hébert PC, Fergusson DA, et al. Age of transfused blood in critically ill adults. N Engl J Med 2015;372:1410-8.

7. Steiner ME, Ness PM, Assmann SF, et al. Effects of red-cell storage duration on patients undergoing cardiac surgery. N Engl J Med 2015;372:1419-29.

8. Guide to the preparation, use and quality assurance of blood components - 18th Edition | EDQM [Internet]. Strasbourg: Council of Europe; 2015 [cited 2016 Jun 15]. Available from: https://www.edqm.eu/en/news/guide-preparation-use-and-quality-assurance-blood-components-18th-edition.

9. BEST (Biomedical Excellence for Safer Transfusion) Committee report on red blood cell recovery standards [Internet]. Bethesda (MD): Blood Products Advisory Committee; 2008 [cited 2016 Jun 13]. Available from: http://www.fda.gov/ohrms/dockets/ac/08/briefing/2008-4355B1_1).htm.

10. Klein HG, Anstee DJ. Transfusion of red cells. In: Mollison's blood transfusion in clinical medicine. 11th ed. Hoboken (NJ): Blackwell Publishing Ltd; 2005. p. 362-73.

11. Zimring JC. Established and theoretical factors to consider in assessing the red cell storage lesion. Blood 2015;125:2185-90.

12. D'Alessandro A, Kriebardis AG, Rinalducci S, et al. An update on red blood cell storage lesions, as gleaned through biochemistry and omics technologies. Transfusion 2015;55:205-19.

13. Perrotta S, Gallagher PG, Mohandas N. Hereditary spherocytosis. Lancet Lond Engl 2008;372:1411-26.

14. Mohandas N, Clark MR, Jacobs MS, et al. Analysis of factors regulating erythrocyte deformability. J Clin Invest 1980;66:563-73.

15. Waugh RE, Narla M, Jackson CW, et al. Rheologic properties of senescent erythrocytes: loss of surface area and volume with red blood cell age. Blood 1992;79:1351-8.

16. Waugh RE, Sarelius IH. Effects of lost surface area on red blood cells and red blood cell survival in mice. Am J Physiol 1996;271:C1847-52.

17. Murdock RC, Reynolds C, Sarelius IH, et al. Adaptation and survival of surface-deprived red blood cells in mice. Am J Physiol Cell Physiol 2000;279:C970-80.

18. Haradin AR, Weed RI, Reed CF. Changes in physical properties of stored erythrocytes relationship to survival in vivo. Transfusion 1969;9:229-37.

19. Safeukui I, Buffet PA, Deplaine G, et al. Quantitative assessment of sensing and sequestration of spherocytic erythrocytes by the human spleen. Blood 2012;120:424-30.

20. Piety N, Reinhart WH, Pourreau PH, et al. Shape matters: the effect of red blood cell shape on perfusion of an artificial microvascular network. Transfusion 2016;56:844-51.

21. Bessis M. Red cell shapes. An illustrated classification and its rationale. Nouv Rev Fr Hematol 1972;12:721-45.

22. Piety NZ, Gifford SC, Yang X, et al. Quantifying morphological heterogeneity: a study of more than 1 000 000 individual stored red blood cells. Vox Sang 2015;109:221-30.

23. Bessis M, Mohandas N, Feo C. Automated ektacytometry: a new method of measuring red cell deformability and red cell indices. Blood Cells 1980;6:315-27.

24. Parpart AK, Lorenz PB. The osmotic resistance (fragility) of human red cells. J Clin Invest 1947;26:636-40.

25. Erdbrügger U, Rudy CK, Etter ME, et al. Imaging flow cytometry elucidates limitations of microparticle analysis by conventional flow cytometry. Cytometry A 2014;85:756-70.

26. Linderkamp O, Wu PY, Meiselman HJ. Geometry of neonatal and adult red blood cells. Pediatr Res 1983;17:250-3.

27. Headland SE, Jones HR, D'Sa AS, et al. Cutting-edge analysis of extracellular microparticles using ImageStream(X) imaging flow cytometry. Sci Rep 2014;4:5237.

28. Berezina TL, Zaets SB, Morgan C, et al. Influence of storage on red blood cell rheological properties. J Surg Res 2002;102:6-12.

29. Blasi B, D'Alessandro A, Ramundo N, et al. Red blood cell storage and cell morphology. Transfus Med Oxf Engl 2012;22:90-6.

30. Mustafa I, Al Marwani A, Mamdouh Nasr K, et al. Time dependent assessment of morphological changes: leukodepleted packed red blood cells stored in SAGM. BioMed Res Int 2016;2016:4529434.

31. Morel FM, Baker RF, Wayland H. Quantitation of human red blood cell fixation by glutaraldehyde. J Cell Biol 1971;48:91-100.

32. Squier CA, Hart JS, Churchland A. Changes in red blood cell volume on fixation in glutaraldehyde solutions. Histochemistry 1976;48:7-16.

33. Eskelinen S, Saukko P. Effects of glutaraldehyde and critical point drying on the shape and size of erythrocytes in isotonic and hypotonic media. J Microsc 1983;130:63-71.

34. Reinhart WH, Piety NZ, Deuel JW, et al. Washing stored red blood cells in an albumin solution improves their morphologic and hemorheologic properties. Transfusion 2015;55:1872-81.

35. Safeukui I, Buffet PA, Perrot S, et al. Surface area loss and increased sphericity account for the splenic entrapment of subpopulations of Plasmodium falciparum ring-infected erythrocytes. PLoS One 2013;8:e60150.

36. Jauréguiberry S, Ndour PA, Roussel C, et al. Postartesunate delayed hemolysis is a predictable event related to the lifesaving effect of artemisinins. Blood 2014;124:167-75.

37. Samsel L, McCoy JP. Imaging flow cytometry for the study of erythroid cell biology and pathology. J Immunol Methods 2015;423:52-9.

38. Laczkó J, Szabolcs M, Jóna I. Vesicle release from erythrocytes during storage and failure of rejuvenation to restore cell morphology. Haematologia (Budap) 1985;18:233-48.

39. Hess JR. Red cell changes during storage. Transfus Apher Sci 2010;43:51-9.

40. Picot J, Ndour PA, Lefevre SD, et al. A biomimetic microfluidic chip to study the circulation and mechanical retention of red blood cells in the spleen. Am J Hematol 2015;90:339-45.

41. Mollison PL. Further observations on the normal survival curve of 51 Cr-labelled red cells. Clin Sci 1961;21:21-36.

42. Lutz HU, Bogdanova A. Mechanisms tagging senescent red blood cells for clearance in healthy humans. Front Physiol 2013;4:387

43. Anniss AM, Sparrow RL. Expression of CD47 (integrin-associated protein) decreases on red blood cells during storage. Transfus Apher Sci 2002;27:233-8.

44. Burger P, Hilarius-Stokman P, de Korte D, et al. CD47 functions as a molecular switch for erythrocyte phagocytosis. Blood 2012;119:5512-21.

45. Bosman GJ, Cluitmans JC, Groenen YA, et al. Susceptibility to hyperosmotic stress-induced phosphatidylserine exposure increases during red blood cell storage. Transfusion 2011;51:1072-8.

46. Burger P, Kostova E, Bloem E, et al. Potassium leakage primes stored erythrocytes for phosphatidylserine exposure and shedding of pro-coagulant vesicles. Br J Haematol 2013;160:377-86.

47. Mittag D, Sran A, Chan KS, et al. Stored red blood cell susceptibility to in vitro transfusion-associated stress conditions is higher after longer storage and increased by storage in saline-adenine-glucose-mannitol compared to AS-1. Transfusion 2015;55:2197-206.

48. Sosale NG, Rouhiparkouhi T, Bradshaw AM, et al. Cell rigidity and shape override CD47's "self"-signaling in phagocytosis by hyperactivating myosin-II. Blood 2015;125:542-52.

49. Prudent M, Tissot JD, Lion N. In vitro assays and clinical trials in red blood cell aging: lost in translation. Transfus Apher Sci 2015;52:270-6.

50. Buffet PA, Milon G, Brousse V, et al. Ex vivo perfusion of human spleens maintains clearing and processing functions. Blood 2006;107:3745-52.

51. Deplaine G, Safeukui I, Jeddi F, et al. The sensing of poorly deformable red blood cells by the human spleen can be mimicked in vitro. Blood 2011;117: e88-95. ◐

SUPPORTING INFORMATION

Additional Supporting Information may be found in the online version of this article at the publisher's website:

Fig. S1. Typical evolution of the projected surface area of RBC at D3 (red histogram), D7 (blue line) and D14 (grey line) of storage.